

Nonequilibrium magnetic dynamics in mechanically alloyed materials

J. A. De Toro, M. A. López de la Torre,* M. A. Arranz, and J. M. Riveiro
Departamento de Física Aplicada, Universidad de Castilla-La Mancha, 13071 Ciudad Real, Spain

J. L. Martínez
Instituto de Ciencia de Materiales, CSIC Cantoblanco, 28049 Madrid, Spain

P. Palade and G. Filoti
National Institute for Physics of Materials, Ro-76900 Bucharest-Magurele, Romania
 (Received 10 April 2000; revised manuscript received 5 March 2001; published 15 August 2001)

The magnetically glassy behavior of mechanically alloyed $\text{Fe}_{61}\text{Re}_{30}\text{Cr}_9$ is reported in detail, including a static and dynamic study of the freezing process, the observation of aging in a mechanically alloyed sample, Mössbauer analysis, and annealing experiments. Despite the clear collective character of the low-temperature change of regime, no thermodynamical spin-glass mean-field transition could be proved. On the other hand, the careful comparison of the magnetic behavior with that reported in strongly interacting fine particles systems hinted towards the presence of that kind of particles in our samples. Structural considerations based on XRD, Mössbauer, and the evolution of the ac susceptibility peaks upon annealing pointed to the existence of very fine Fe-rich clusters able to support a magnetic moment, confirming the diagnosis extracted from the magnetic dynamics analysis. The argument is strengthened by the study of the effects of milling on the freezing temperature in a second sample showing a similar behavior: $\text{Fe}_{35}\text{Al}_{50}\text{B}_{15}$. The explanation can be extended naturally to previously reported mechanically alloyed, spin-glass-like samples, which hints towards the generalization of our interpretation.

DOI: 10.1103/PhysRevB.64.094438

PACS number(s): 75.50.Lk, 75.50.Kj, 75.50.Tt, 75.40.Cx

I. INTRODUCTION

Ball milling or mechanical attrition is a well-established technique for the synthesis of a variety of metastable phases, such as extended solid solutions, alloys of immiscible elements, amorphous alloys, or quasicrystalline phases.¹ Essentially, the disordering and alloying of the different species take place at the grains interfaces due to the high shear rate induced by the balls collisions. Depending on the type of starting constituents, two main procedures can be distinguished: in *mechanical alloying* (MA), the departing constituents are two or more elemental powders, whereas the term *mechanical milling* (MM) refers to the milling of intermetallic compounds (or, sometimes, a single elemental powder). Both methods have been recently found to be capable of producing novel spin glasses (SG),²⁻⁵ often with a surprisingly high concentration of the magnetic elements, i.e., *concentrated* spin glasses. It is remarkable that these rather crude techniques may produce such a subtle magnetic phase. As far as MM is concerned, Klein⁶ suggested a superparamagnetic-like blocking of magnetic particles to explain what Zhou and Bakker claimed a true spin glass in a MM nanocrystalline Gd-Al Laves phase.³ Hernando *et al.* pointed out another possibility to explain the spin-glass-like (SGL) behavior of nanocrystalline samples: spin disorder at the nanocrystals boundaries.⁷ Although the chemical and/or site disorder can theoretically justify the existence of competing interactions leading to the appearance of a SG phase, no thermodynamic phase transition has been demonstrated so far in any of the referred samples, therefore leaving the question open to further research. The same is applicable to the spin-glass-like MA materials, on which this paper will be

focused, where the interpretation is often more difficult due to the presence of different structural and magnetic phases.⁸

The possible presence of a SG phase in mechanically alloyed materials has been expressed in some recent works.^{5,8} Other MA products, such as the much-studied Co-Cu, have resulted in superparamagnetic behavior.⁹ In a previous paper, some of us found distinctive spin glass ac and dc susceptibility features in a MA $\text{Al}_{49}\text{Fe}_{30}\text{Cu}_{21}$ nanocrystalline alloy¹⁰ (sample AFC), but could not observe the SG typical divergence of the nonlinear susceptibility (χ_{nl}).¹¹ Other magnetic properties [the thermal hysteresis between the zero-field cooled (ZFC) and the field cooled (FC) magnetization, the frequency-dependent cusp of the ac susceptibility, or some relaxation features] are not unequivocal, as will be reviewed along this work. The SGL behavior of AFC was then related to the blocking of some interacting magnetic particles, inspired by the results intensively reported in the last few years, both experimental¹²⁻¹⁴ and theoretical,¹⁵ on the spin glass behavior of fine ferromagnetic particles systems with strong dipole interaction. The study of the effects of interparticle interactions is also relevant in the context of giant magnetoresistive granular materials.¹⁶ The present work does not simply present two more examples of SGL behavior in MA samples, but aims to settle the issue and controversies in this kind of materials by clarifying some uncertain aspects in Ref. 10: (i) the cooperative dynamics below the freezing temperature is proved with the neat observation of *aging* phenomena for the first time, to the best of our knowledge, in an alloy synthesized by MA [before, Bonetti *et al.* had reported it in MM nanocrystalline pure Fe (Ref. 17)] and (ii) the underlying microstructure is investigated by contrasting low temperature Mössbauer data with the structural picture

suggested by the magnetic analysis. Additionally, the comparison of the results presented here with those reported in AFC (Ref. 10) and FWA (Ref. 18) will allow us to tentatively generalize the explanation for the SGL behavior in MA materials.

Most of the paper is concerned with a $\text{Fe}_{61}\text{Re}_{30}\text{Cr}_9$ alloy (FRC), whose low-temperature magnetic dynamics has been thoroughly analyzed. Samples at different milling times were studied in the system $\text{Fe}_{35}\text{Al}_{50}\text{B}_{20}$ (FAB) in order to achieve better structural insight. Instead of the more usual presentation where structural considerations precede the magnetic properties account, the paper is organized in the opposite way. This is done so in order to emphasize how the analysis of the magnetic behavior in this kind of materials can be used to diagnose the structure responsible for such behavior, which, in addition, appears certainly hard to determine by conventional structural probes (XRD or HRTEM).

II. EXPERIMENTAL

The samples were obtained by mechanical alloying elemental powders in a conventional high-energy planetary mill operating at 225 rpm. The powders were sealed under an Ar atmosphere in hardened steel pots with the 20% of their volumes occupied by 10 mm \varnothing balls of the same material. The ball-to-powder mass ratio was kept approximately equal to 12:1. These are the same conditions employed to synthesize the samples AFC (Ref. 10) and FWA.¹⁸ The composition and structure evolution were followed throughout the milling by x-ray energy dispersive spectroscopy (XEDS) and x-ray diffraction (XRD), respectively. The latter was accomplished using $\text{CuK}\alpha$ radiation, 2θ geometry and integration times as high as 20 s in a MPD Philips diffractometer. The structure of FRC was further investigated by high resolution transmission electron microscopy (HRTEM) and selected-area electron-diffraction (SAED). Mössbauer spectra of the same material were recorded at $T=300, 80,$ and 15 K in a closed-cycle cryostat using a standard Mössbauer setup with symmetrical wave form. The FRC annealed samples were obtained by heating during 10 h at 300 and 400 °C in a high vacuum furnace.

Hysteresis loops at various temperatures were registered with a vibrating sample magnetometer (VSM) equipped with a He cryostat. A Quantum Design SQUID magnetometer was employed to measure dc magnetization (FC and ZFC runs) and, in the case of FRC, ac susceptibility in the temperature range 4.2–200 K for different values of applied dc magnetic field and frequency. The aging experiment was performed in the same apparatus as follows: the sample was first cooled from room temperature down to the magnetically *glassy* regime, then it was allowed to age for a waiting time t_w before applying a small external dc field ($H = 10$ Oe) and register the isothermal time evolution of the magnetization. This procedure was repeated for different t_w keeping the same cooling rate. The ac susceptibility vs temperature curves in the FAB samples were recorded using the conventional mutual-inductance method in a homemade susceptometer built in a closed cycle helium cryostat; those of FRC were measured in a SQUID magnetometer in order to obtain better resolved

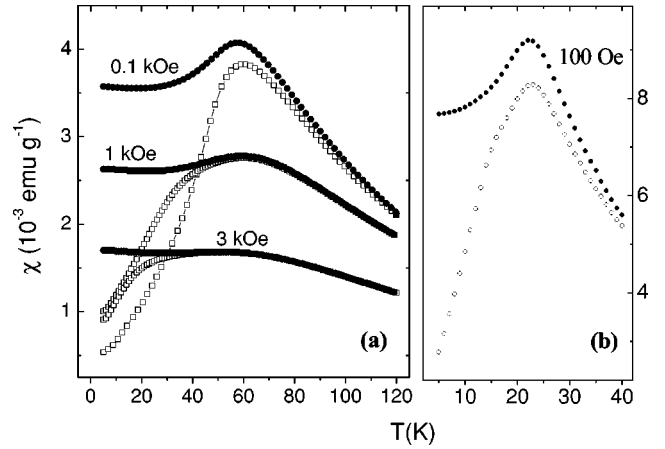


FIG. 1. Zero-field-cooled (open squares) and field-cooled (solid circles) magnetization measured with fields $H=100, 1000,$ and 3000 Oe for FRC (a) and with $H=100$ Oe for FAB (b).

data for use in the dynamic scaling and critical slowing down analysis.

III. RESULTS AND DISCUSSION

A. Magnetic characterization

After milling for 460 h the XRD patterns and room temperature magnetization showed no significant changes. The composition of this final product (FRC), as measured by EDAX, was $\text{Fe}_{61}\text{Re}_{30}\text{Cr}_9$, revealing Fe and Cr enrichment due to the Re abrasive action upon the milling tools. On the other hand, the nominal composition of FAB was not significantly altered. In the following, FAB will stand for the material obtained after 440 h of milling, although samples milled for different times will be also discussed for comparison. Figure 1(a) shows selected FC and ZFC susceptibility ($\chi=M/H$) curves for FRC measured at different H . With decreasing H the irreversibility between these curves begins at higher temperatures and the smooth maximum in the FC branch becomes more pronounced, whereas higher H yields blunter ZFC maxima shifting to lower temperatures. The irreversibility temperature T_{irr} approaches the ZFC maximum temperature $T_{\text{max}} \approx 60$ K in parallel with the progressive smearing out of the smooth FC peak. The same aspects are observed for FAB [see Fig. 1(b) for $H=100$ Oe and focusing on the irreversible region], except for the lower temperature of the ZFC maximum $T_{\text{max}} \approx 30$ K. The strong thermomagnetic irreversibility mixes features from the superparamagnetic and the spin-glass typical irreversibilities. It recalls the former in the rather broad ZFC peak and in the fact that, for low H , the FC branch separates from the ZFC one. The quantities T_{max} and T_{irr} [defined as the temperature at which $\chi_{\text{FC}} - \chi_{\text{ZFC}}$ equals 10% of $\chi_{\text{ZFC}}(T_{\text{max}})$] can give, following Hansen and Morup,¹⁹ a quick estimate of an assumed log-normal distribution of superparamagnetic particles, where the width of the distribution σ increases with $T_{\text{irr}}/T_{\text{max}}$. Such estimation leads for FRC and FAB to extremely narrow size distributions [χ_{ZFC} does not even depart a 10% of $\chi_{\text{ZFC}}(T_{\text{max}})$ from χ_{ZFC}], which, taking into account

the crude synthesis method employed, indicates the inadequacy of the superparamagnetic approach. On the other hand, the thermomagnetic irreversibility in Fig. 1 resembles that of spin glasses in the plateaulike shape of the FC curve below T_{\max} (in superparamagnets the FC branch keeps increasing monotonously²⁰). However, this feature has been recently found not to be exclusive of SG, but also shared by fine particle systems with random anisotropy and strong dipole-dipole interaction.^{13,21} Such was reported from a Monte Carlo simulation where it was also shown that the particles size distribution does not affect such behavior.¹⁵ It must be remarked that the thermal irreversibility commented here is essentially the same as those reported for AFC (Ref. 10) and FWA.¹⁸

The analysis of the frequency and temperature dependence of χ_{ac} in FRC led to a similar mixture of spin glass and superparamagneticlike features, suggesting again the picture of fine particles with strong interaction (comparable or higher than the particle anisotropy barrier $E_b = KV$, where K is some effective anisotropy constant). In principle, the interparticle interaction may be either dipolar or RKKY in origin, for both of them can provide the necessary competing spin alignment, which, together with spatial disorder, yields frustration for some of the moments. The frequency dependence of the in-phase χ' and out-of-phase χ'' linear ac susceptibility for FRC is shown in Figs. 2(a) and 2(b), respectively, in the interesting temperature range. The χ' peak temperatures $T_{\max}(\omega)$, are consistent with the lower dc value from the ZFC maximum. When the frequency increases, $T_{\max}(\omega)$ shifts rightwards and the height of the susceptibility peak diminishes, both neatly but slightly. These features are customarily found in canonical spin glasses.²² Furthermore, the peak strongly smears out and shifts to lower temperatures when moderate external dc fields are applied (not shown for FRC, see the analogous behavior of AFC in Ref. 10). Although the inflection points of χ' for the different frequencies approximately coincide with the absorption maxima as predicted by the Casimir–du Pré equations²² [see inset in Fig. 2(a)], the shape of the latter is Lorentzian in contrast with the abrupt onset of dissipation found in canonical spin glasses²² and similarly to what has been observed in interacting nanoparticles.^{14,23} The value of the frequency sensitivity (relative variation of the peak temperature per decade frequency) is $p \approx 0.02$, far smaller than the sensitivity exhibited by thermally activated processes and falling in the same range of metallic spin glasses values. Concerning the functional dependence of $T_{\max}(\omega)$, neither the Néel-Arrhenius ($\omega/\omega_0 = \exp[-E_a/kT]$) nor the Vogel-Fulcher laws (which substitutes T by $T - T_0$ in the exponential above, being T_0 an “interaction temperature”) yielded physical values for the fitting parameters. The latter of these thermally activated dynamics laws has been shown successful to describe the dynamics of particle systems with *weak* dipolar interaction.²⁴ On the other hand, the analogy with assemblies of strongly interacting particles is illuminating: remarkably, Fig. 2 mimics the temperature and frequency behavior of both χ' and χ'' reported by Jönsson *et al.* in dense frozen ferrofluids,¹⁴ an *a priori* completely different scenario. In particular, the absorption [Fig. 2(b)] is nearly frequency independent for tem-

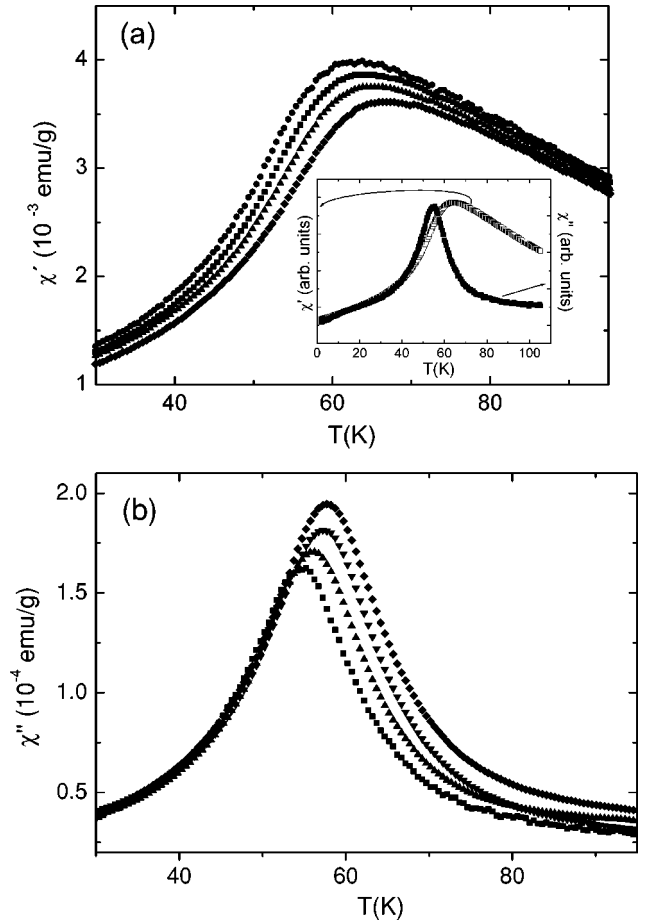


FIG. 2. Real (a) and imaginary (b) components of the ac susceptibility vs temperature in FRC for different frequencies: 10 Hz (●), 100 Hz (■), 1 kHz (▲), 5 kHz (▼), and 10 kHz (◆). The inset in (a) shows both components for easier comparison.

peratures below T_{\max} , meaning that the distribution function of relaxation times $g(\tau)$ remains essentially invariable with frequency, which gives to T_{\max} the character of a *freezing* temperature.

It must be pointed out, however, that the analysis of the frequency dependence may be useful to compare a number of systems,²⁵ but nothing can be definitely concluded about the possible existence of a true phase transition²² taking place at a finite temperature. This possibility was explored in FRC by both investigating the temperature behavior of the nonlinear magnetic susceptibility χ_{nl} (Ref. 26) and by searching for a meaningful dynamic scaling.²⁷ For the $\chi_{nl}(T)$ analysis, FC data measured with fields ranging from 0.1 to 1.5 kOe was used to extract isothermal $M(H)$ curves, which were then fitted to the expression $M = m_0 + \chi_0 H - b_3(\chi_0 H)^3 + b_5(\chi_0 H)^5$. The results are not shown since their features are the same as in AFC:¹⁰ $b_3\chi_0^3$, the first nonlinear coefficient, shows a broad maximum at T_f , but the normalized, more significant, coefficient b_3 does not exhibit any increase that could recall its typical divergence in canonical spin glasses. Some more discussion and details on the fitting procedure can be seen in Ref. 10. The curve $\chi_0(T)$ obtained from the fit starts departing considerably from the

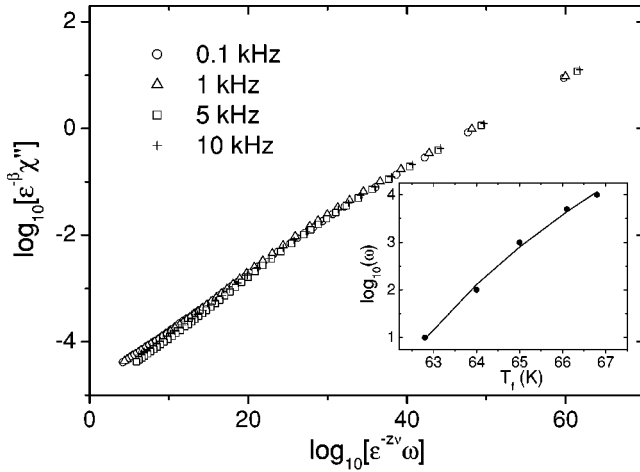


FIG. 3. Scaling of the imaginary susceptibility of FRC obtained for $T_c = 58$ K, $\beta = 2$, and $z\nu = 24$. The inset shows the fit to the critical slowing down law, which yielded a different value for $z\nu = 11 \pm 5$.

Curie-Weiss law well above the freezing temperature, indicating the presence of interactions between the hypothetical particles.

If a transition to a spin-glass state existed at $T_f \sim T_{\max}$, it has been established²⁸ that the out-of-phase component of the susceptibility could be scaled as

$$\chi''(T, \omega) = \epsilon^\beta F(\omega \epsilon^{-z\nu}), \quad (1)$$

where ϵ is the reduced temperature, $\epsilon = (T - T_c)/T_c$, β is the critical exponent describing how the order parameter would approach zero at T_c , ν is the critical exponent for the correlation length $\xi \sim \epsilon^\nu$, and z is the exponent relating the relaxation time $\tau \sim 1/\omega$ with ξ . The best scaling (shown in Fig. 3) is obtained for $T_c = (58 \pm 1)$ K, $\beta = 2.0 \pm 0.3$, and $z\nu = 24 \pm 3$. No satisfactory data collapse could be achieved for exponent values closer to those typically reported in the spin-glass literature.²² This large departure of the hypothetical critical exponents from the physical values have been found before in magnetic cluster systems, such as Mn-rich Cu-Al-Mn shape memory alloys²⁹ or Fe grains dispersed in an alumina matrix.³⁰ The fit to the critical slowing down law for the relaxation time $\tau \sim [(T - T_c)/T_c]^{-z\nu}$ was performed using $T = T_{\max}(\omega)$, and yielded the exponent $z\nu = 11 \pm 5$ (see inset in Fig. 3). Although still high, this is a credible value. However, given the unrealistically high value obtained for β and, more importantly, that different results for $z\nu$ are obtained with different computing methods, we ratify with ac analysis that there is no spin-glass phase transition in FRC.

Therefore, while $\chi(H, T, \omega)$ displays the characteristic signature of critical fluctuations at a paramagnetic-spin-glass phase transition, both dc and ac critical behavior analysis have failed to satisfy the quantitative predictions of the mean-field model. The freezing of fine strongly interacting particles, as hinted along this work, would account for the close SGL behavior and the failure to undergo a phase transition due to the moment size distribution.¹⁴ This picture is strengthened by the observation of aging phenomena, an un-

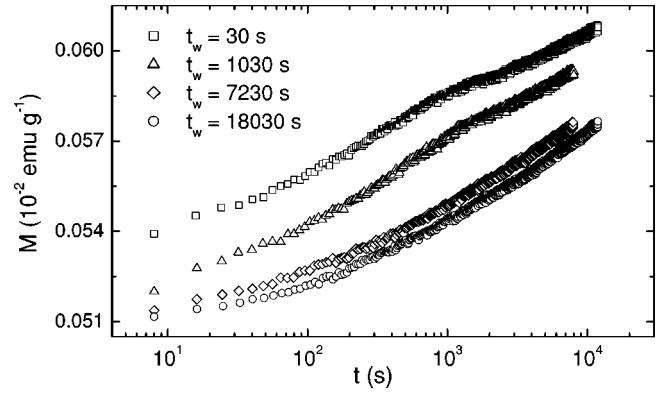


FIG. 4. Time dependence of the zero-field-cooled magnetization measured at $T = 40$ K in FRC for four different waiting times t_w before the application of $H = 10$ Oe.

equivocal sign of collective dynamics, for it is well explained both by mean-field theories (as a consequence of the chaotic nature of the multivalley free energy) and by the droplet model.³¹ As far as we know, Fig. 4 presents the first report of aged magnetic relaxation in a mechanically alloyed material. The $M(t)$ curves (registered as described in the experimental section) are clearly dependent on the elapsed time t_w before applying the magnetic field H . This is conclusive in asserting chaotic correlated dynamics against individual particle relaxation, consistently with the above commented failure of thermally activated dynamics laws. Care was taken in this experiment in avoiding thermal history variations between the measurement for each t_w , as this has been recently shown to influence significantly the response function,³² especially for short t_w . Other features to be noticed in Fig. 4 are the usual logarithmic dependence of the relaxation and the decreasing magnetization for increasing t_w . The wait time dependence of the relaxation is weaker than in spin glasses²⁷ and similar to that recently reported by Djurberg *et al.* for dense frozen ferrofluids.³³ The aging effect was considerably diminished for $T = 60$ K (not shown), and no relaxation was observed at higher temperatures. It must be made clear that aging effects can be observed in inhomogeneous freezing processes taking place without the occurrence of a true SG phase transition, as it has recently been explained more explicitly by Fiorani *et al.* for $\gamma\text{-Fe}_2\text{O}_3$ nanoparticles.³⁴ Measurements to test aging phenomena in other MA samples are projected, although its existence seems likely from the parallelisms in the other dynamical features.

So far we have diagnosed the existence of some magnetic particles, which interact strongly at low temperatures, embedded in a nonferromagnetic medium, namely, the paramagnetic alloy with overall composition around $\text{Fe}_{61}\text{Re}_{30}\text{Cr}_9$. The paramagnetic character of this matrix can be reasonably understood in terms of the Re efficiency to weaken the Fe magnetic moments upon dilution.³⁵ The structural origin of the ferromagnetic particles will be addressed in the following section. An estimation of the mean moment size was obtained from the magnetization curve $M(H)$ at 200 K, shown in Fig. 5. The nonsaturating behavior reveals the presence of a superparamagnetic phase. A small ferro-

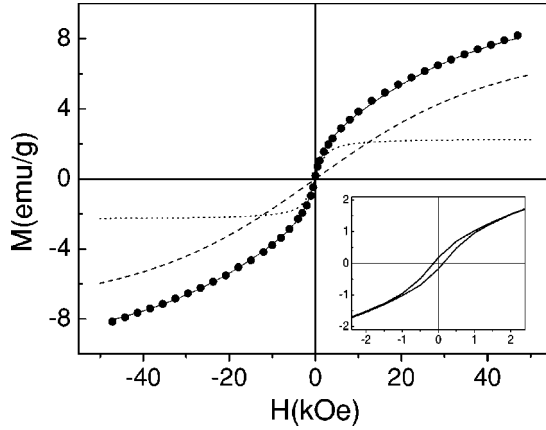


FIG. 5. Hysteresis loop for FRC measured at $T=200$ K. The solid line is the fit to the left branch of the loop as explained in the main text. The dashed and dotted lines are, respectively, the superparamagnetic and the ferromagnetic contributions. The inset focuses at lower fields to show the presence of hysteresis in the loop.

magnetic contribution, arising from larger, blocked, particles (probably coming from late contamination from the milling tools), is evidenced by the small hysteresis loop, justifying the use of relatively high fields (higher than the ferromagnetic saturation value) for the above $\chi_{nl}(T)$ analysis. At 200 K the interaction between particles can be neglected, as it is confirmed by the Curie-Weiss behavior of the susceptibility, and a superparamagnetic model is a good approximation to describe the sample magnetization. Higher values of the temperature would result in larger errors in the superparamagnetic fitting parameters, for this contribution would appear just linear. The cycle was fitted to the expression used by Stearns and Cheng³⁶

$$M(H) = M_{FM} + M_{SPP} = \frac{2M_{FM}^s}{\pi} \tan^{-1} \left[\frac{H \pm H_c}{H_c} \tan \left(\frac{\pi S}{2} \right) \right] + N\mu \left[\coth \left(\frac{\mu H}{kT} \right) - \left(\frac{\mu H}{kT} \right)^{-1} \right] \quad (2)$$

where μ is some mean moment and N the number of particles per gram. Including an extra paramagnetic term did not improve the quality of the fit. In any case, we have estimated an upper limit for the paramagnetic susceptibility to be about 5×10^{-6} emu/g, less than a 3% contribution to the magnetization at 5 T.³⁷ The fit (shown in Fig. 5 together with the separate contributions) is reasonably good considering that no particle size distribution was taken into account. The size of the mean moment is as small as $\mu = (174 \pm 7) \mu_B$, which would correspond to spherical pure bcc Fe clusters with approximately 4 atoms of diameter (~ 1 nm), difficult indeed to detect by either XRD or conventional HRTEM in a bulk sample (in addition, the particles or clusters would presumably consist of a highly disordered Fe-rich alloy and not pure Fe). From the saturation value of the superparamagnetic component, $N\mu = (9.0 \pm 0.1)$ emu/g, and assuming the bulk magnetic moment of Fe, the fraction of Fe atoms in the form

of clusters is estimated to be $(11 \pm 1)\%$, in good agreement with the value obtained below from Mössbauer spectroscopy. From this fraction, it follows that the volume concentration (around 10%), given the small cluster moment, is not enough to produce a significant dipolar interaction. Consequently, the dipolar interaction can be ruled out as responsible for the here studied low temperature SGL behavior. Larger particles and higher densities are indeed necessary in the referred frozen ferrofluids in order to achieve SGL behavior. Hence, the main interaction between clusters must be RKKY-type, mediated by the conduction electrons in the supersaturated solid solution.

Although most of the discussion so far has been done for FRC, we must emphasize that FAB, AFC, and FWA share every feature reported here for FRC, most importantly the presence of dc thermoirreversibility as described above, and the slight frequency sensitivity of the ac susceptibility peak. A discordant particularity is found in the sudden onset of the adsorption in AFC (Ref. 10) (instead of the usual Lorenzian). Despite the variety of materials employed, a correlation between the Fe concentration and T_{\max} appears straightforward, since AFC, FWA, and FAB (with 30% at. of Fe) have T_{\max} around 25 K, whereas FRC, which is much richer in Fe, shows $T_{\max} = 60$ K. In fact, if fine monodomains due to compositional clustering were to remain embedded in a paramagnetic saturated solution, they would be naturally expected to be larger and/or more numerous with increasing Fe concentration. In SGL particle systems T_{\max} is known to increase with the size of the moments and the intensity of the interactions between them,¹⁶ both variables being favored by the increase of Fe. Similarly, compositional clustering might be relevant as well in the work of Tang *et al.*, who claimed to have found a spin glass phase in a mechanically alloyed $\text{Ag}_{85}\text{Gd}_{15}$ supersaturated solid solution on the basis of ZFC and FC measurements.⁵ On the other hand, Galdeano *et al.* have recently investigated the effect of milling intensity and temperature on the final nanostructure of MA $\text{Cu}_{87}\text{Fe}_{13}$, and still found, at this lower concentration of Fe, the coexistence of very small Fe-rich clusters with larger particles and a solid solution.⁸ When tackling the interpretation of the magnetic properties in a structurally similar sample they comment the difficulties to “make the difference between very small interacting particles and a solid solution.” A more systematic sweep of Fe concentration in different systems is projected in order to confirm the universality of the *nanoparticle glass* behavior in MA materials.

B. Structural considerations

The evolution of the XRD patterns with milling time for FRC and FAB was similar to that shown for AFC.¹⁰ The minor peaks progressively disappear whereas the larger reflections (around $2\theta = 40^\circ$) broaden and eventually collapse into a quite symmetric nanocrystalline peak. The width of such peak is larger than 5° at half maximum for both samples. In some occasions, such wide peaks have been taken as amorphous halos,³⁸ setting a misleading structural basis for subsequent magnetic interpretation. In this respect, the observation of crystallization peaks by calorimetric techniques does not guarantee the absence of nanoscale grains or compositional clustering, which may be transcendental in the

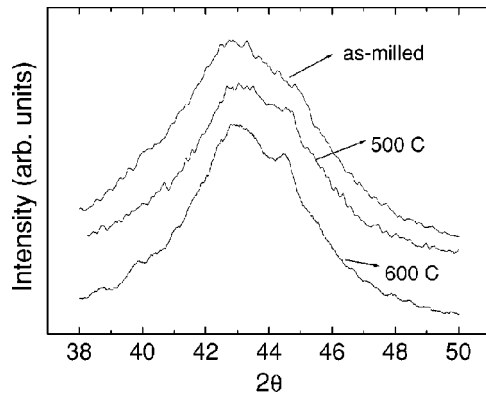


FIG. 6. Detail of the XRD patterns for FRC as-milled and annealed at 500 and 600 °C.

context of glassy magnetic materials. Figure 6 focuses on the only remaining peak in the XRD pattern after nearly two weeks of milling, and the changes it undergoes upon annealing as described in the experimental section. The as-milled peak is centered close to the main hcp-Re reflection, pointing to the existence of very fine Re-rich nanocrystals. Preliminary HRTEM results confirmed the presence of nanocrystals embedded in a majority amorphous phase. The electron diffraction micrograph indicating so is analogous to that for AFC (annular ring around a large diffuse halo).⁹ Attempts to observe compositional clustering were unproductive. More specific high-resolution methods are needed for this purpose, for instance, Lewis *et al.* announced very recently that they were able to observe Fe clusters with a diameter of approx. 50 atoms in a bulk sample using conical dark-field imaging techniques.³⁹ However, the XRD broad peak in the as-milled sample is not symmetric, but a slight hump can be noticed about $2\theta = 44.5^\circ$, near the $\langle 100 \rangle$ bcc-Fe position, suggesting the presence of some Fe-rich nanocrystalline regions. Yet, a word of caution must be said about these observations, for Le Caër *et al.* have demonstrated that XRD information in this kind of samples is not very reliable.⁴⁰ In any case, the hump becomes more pronounced after annealing at 500 °C, and shapes as a peak for 600 °C, indicating Fe aggregation from the paramagnetic supersaturated amorphous solid solution matrix and strengthening the hypothesis of the existence of Fe-rich nucleation sites in the as-milled material. Annealing at $T < 500^\circ\text{C}$ had barely noticeable effects in the XRD patterns, which were always obscured by the presence of the Re-rich nanocrystals, however, the ac susceptibility technique proved very sensitive to annealing at these temperatures. Figure 7 displays the χ' vs T curves, measured at 100 Hz, for the as-milled, 300 °C annealed and 400 °C annealed samples. A clear shift towards higher temperatures for increasing temperatures signals the growth of the Fe-rich clusters. For higher temperatures, the peak was progressively overshadowed by the larger fraction of multidomain particles (no peak was observed for samples annealed at more than 500 °C).

A further demonstration of how magnetic ac susceptibility can be used to gain insight on the issue of nanoscale compositional homogeneity is provided by the following study of the evolution of the low temperature susceptibility peak in

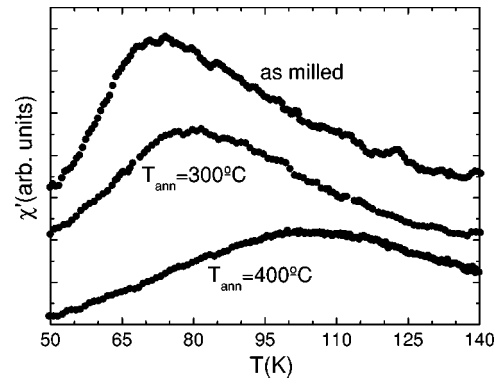


FIG. 7. Real component of the ac susceptibility of as-milled FRC, and after 300 and 400 °C annealing, measured at 100 Hz.

FAB with the milling time. The sample MA for 250 h showed a SGL peak in $\chi'(T)$ sharper than that of FRC, indicating a narrower size distribution of the clusters, which gave more accuracy to the values of the peak temperature (T_p). All peaks showed a similar small frequency sensitivity ($p \approx 0.02$). The points in Fig. 8 (left axis) represent T_p obtained in curves $\chi'(T)$ measured with a frequency of 1 kHz. T_p decreases monotonously since its appearance at 160 h, until it reaches what could be considered a stationary state after 3 weeks of milling. The apparent shift of the peak upon milling can be readily explained by the progressive Fe dilution, which results in even finer clusters with a lower freezing temperature. Therefore, in this final stage of cluster refinement, the effect of milling is just the opposite of the annealing treatments described above: Fe segregation or dilution versus aggregation.

Once the existence of the suggested ultrafine monodomains is assumed, the question arises if they could be related to the nanocrystals revealed by the broad XRD peaks. One may think so given that (i) the size scale of the nanocrystals and the magnetic clusters is roughly the same, (ii) the positions of the XRD peaks ($2\theta = 43.6^\circ$ in FAB and AFC,

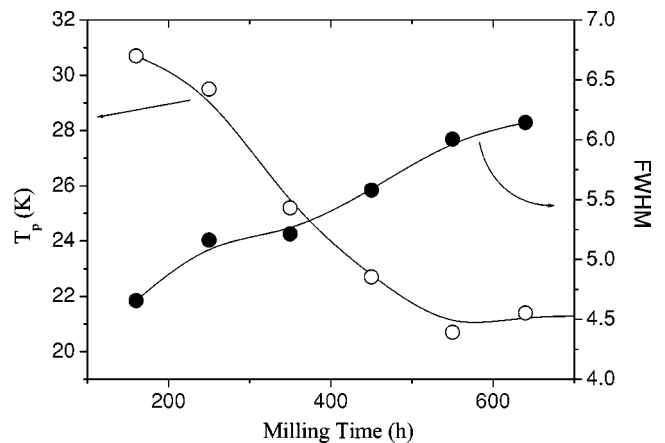


FIG. 8. The left axis shows the temperature of the maximum of the ac susceptibility vs temperature curves (measured at 1 kHz) for the sample $\text{Fe}_{35}\text{Al}_{50}\text{B}_{15}$ at different milling times. The FWHM of the respective XRD peaks is plotted in the right axis. The lines are guides to the eye.

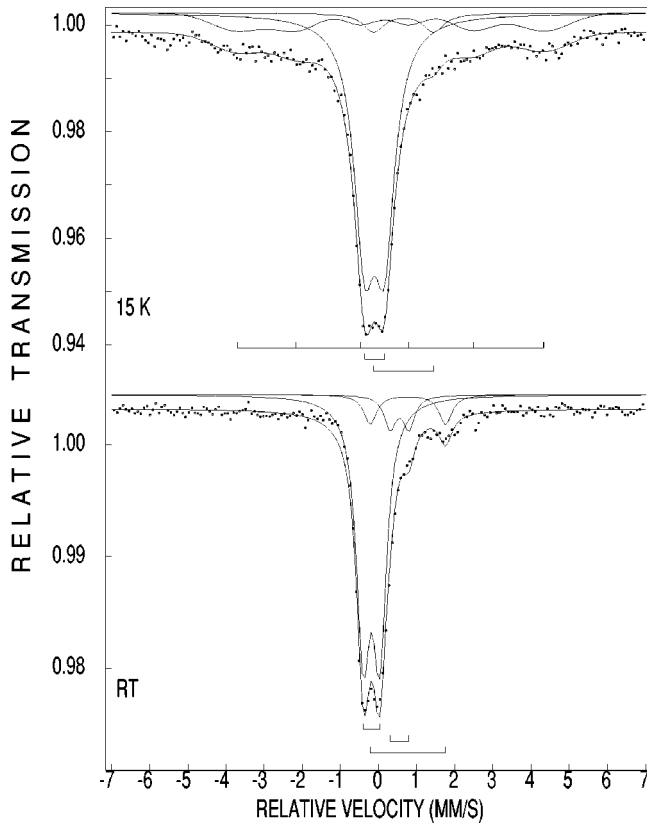


FIG. 9. Mössbauer spectra of FRC at 15 and 300 K, best fitted with three components.

43.3 in FRC) are not far from the bcc-Fe 100 peak, and above all, (iii) the decrease in T_p upon milling, meaning the reduction of the magnetic clusters size, goes together with the refinement of the crystallite size (see Fig. 8). However, this hypothesis vanishes with the comparison of the different Fe-based samples discussed along the paper: the XRD peaks of FRC and FAB have similar widths, but T_{\max} in FAB is half that of FRC; more conclusively, FRC exhibits a much wider XRD peak than AFC (Ref. 10) (FWHM = 5.3 and 2.5, respectively), however T_{\max} is larger in FRC. Indeed, although the loss of crystalline order range upon milling progresses simultaneously with the dilution of Fe, there is no need for the nanocrystallites and the Fe-rich clusters to be spatially related. In particular, for FRC, the broad XRD peak centered at $2\theta=43.3^\circ$ was reasoned above to reflect the presence of Re-rich nanocrystals.

As a final experimental attempt to test the existence of fine compositional clustering leading to magnetic monodomains in FRC, we performed Mössbauer spectrometry at various temperatures between 15 and 295 K. The Mössbauer investigations put in evidence three different configurations of iron in FRC. At room temperature (RT), as illustrated in Fig. 9, the Mössbauer spectrum is fitted using three quadrupolar doublets. The doublet reflecting the highest amount of iron (large majority) showed a quadrupole splitting (QS) of 0.43 mm s^{-1} with an isomer shift (IS), referring to ^{57}Co in Rhodium matrix, of -0.18 mm s^{-1} . There is another doublet with rather big positive $\text{IS}=0.77 \text{ mm s}^{-1}$ and large $\text{QS}=1.97 \text{ mm s}^{-1}$ which could be assigned without any doubts to a

Fe^{2+} specie. The third doublet has the following parameters $\text{QS} = 0.49 \text{ mm s}^{-1}$ and $\text{IS} = 0.55 \text{ mm s}^{-1}$. The spectrum measured at 75 K showed no changes, which ratifies that $T_{\max}=60 \text{ K}$ is not a blocking temperature, since then it would be highly affected by time window effects, but a freezing temperature. The appearance of a sextet with very broad peaks in the lowest temperature spectrum (15 K) indicates the existence of a magnetic ordered phase (see Fig. 9), with a highly disordered structure and/or a large distribution of magnetic interactions (probably both, taking into account the characteristics of the synthesis method). The Mössbauer data point to the third doublet described in the RT spectrum as the one which orders below 60 K. The other two doublets parameters did not show significant change. The area of the Mössbauer components is proportional to the amount of Fe atoms, which are subjected to certain interactions which depend on their particular location in a definite configuration. The change of relative area with temperature among the components is related to variations, either structural or magnetic, in the Fe environment. Structural transformations can be discarded. The strong absorption lines of the central doublet makes difficult to assign the magnetic ordered phase, but, if we consider that the Fe^{2+} species is the result of residual surface oxidation during the intensive ball milling and the central doublet is due to the matrix (an amorphous phase which remains paramagnetic down to at least 15 K, or 5 K if we consider the magnetic data), the magnetic phase appearing at low temperature has to be attributed to the the Fe-rich fine clusters embedded in the majority paramagnetic phase. The good agreement between the area percentage of this phase 8.4% and the fraction of Fe atoms estimated above from the superparamagnetic magnetization at higher temperatures, confirms the adequacy of the data treatment. The magnetic effective field of the sextet measured at 15 K is 25.8 T, too large for a spin glass phase, and consistent with an Fe-rich amorphous or, as the results shown in Fig. 6 suggest, a highly disordered nanocrystalline structure. The large linewidths of the sextet is a consequence of such disorder. Therefore, the Mössbauer study corroborates the whole picture of *nanoparticle glass* obtained from the magnetic dynamics analysis.

IV. CONCLUSIONS

In summary, it has been shown that the spin-glass-like properties of several mechanically alloyed systems with Fe concentration higher than 30% are caused by the freezing of strongly RKKY interacting ferromagnetic clusters, which are embedded in a paramagnetic supersaturated solid solution. We have first arrived to such conclusion by the interpretation of ac and dc magnetization vs temperature data in the light of results obtained in the last few years for strongly dipolarly interacting particles. In the case of FRC, the collective nature of the low-temperature SGL phase has been confirmed with the first measurement of aged relaxation in a MA system. However, the transition failed to satisfy the critical behavior expected for a spin glass due to broad particle size and interaction distributions. The presence of very small particles, rather nanosized *clusters* (around 1 nm of diameter in FRC),

diagnosed from an strictly magnetic dynamics analysis has been then confirmed by structural considerations including the observations, on the one hand, of the growth of the Fe-rich nuclei upon annealing and, on the other hand, the decrease in the ac susceptibility peak, meaning further dilution of the clusters, with the milling time. Mössbauer analysis also ratified the freezing of a highly disordered magnetic phase. The compositional clustering has been argued to be spatially independent of possible residual crystallinity in the samples (separate presence of Re nanocrystals and Fe-rich

magnetic clusters). These arguments have been extended to previously reported samples. Its generalization appears plausible and emphasizes the difficulties to produce nondiluted mechanically alloyed materials with compositional homogeneity down to the atomic scale.

We acknowledge the help of Dr. P. Herrero, from Universidad Complutense de Madrid, and Dr. Altaf Carim, from Pennsylvania State University, in the discussion of the sample structure. This work was supported by the Spanish DGICYT (Grant No. MAT1999-0358).

*Author to whom correspondence should be addressed. Electronic address: malopez@fiap-cr.uclm.es

- ¹C. C. Koch, *Nanostruct. Mater.* **2**, 109 (1993).
- ²G. F. Zhou and H. Bakker, *Phys. Rev. Lett.* **72**, 2290 (1994).
- ³G. F. Zhou and H. Bakker, *Phys. Rev. Lett.* **73**, 344 (1994).
- ⁴D. X. Li, K. Sumiyama, K. Suzuki, and T. Suzuki, *Phys. Rev. B* **55**, 6467 (1997).
- ⁵J. Tang, W. Zhao, C. J. O'Connor, C. Tao, M. Zhao, and L. Wang, *Phys. Rev. B* **52**, 12 829 (1995).
- ⁶L. Klein, *Phys. Rev. Lett.* **74**, 618 (1995); G. F. Zhou and H. Bakker, *ibid.* **74**, 619 (1995).
- ⁷A. Hernando, E. Navarro, M. Multigner, A. R. Yavari, D. Fiorani, M. Rosenberg, G. Filoti, and R. Caciuffo, *Phys. Rev. B* **58**, 5181 (1998).
- ⁸S. Galdeano, L. Chaffron, M.-H. Mathon, G. André, E. Vincent, and C.-H. de Novion, *Mater. Sci. Forum* **343-346**, 715 (2000).
- ⁹I. W. Modder, E. Schoonderwaldt, G. F. Zhou, and H. Bakker, *Physica B* **245**, 363 (1998).
- ¹⁰J. A. De Toro, M. A. López de la Torre, J. M. Riveiro, R. Sáez Puche, A. Gómez-Herrero, and L. C. Otero-Díaz, *Phys. Rev. B* **60**, 12 918 (1999).
- ¹¹J. Souletie and J. L. Tholence, *Phys. Rev. B* **32**, 516 (1985).
- ¹²S. Morup, F. Badker, P. V. Hendriksen, and S. Linderoth, *Phys. Rev. B* **52**, 287 (1995).
- ¹³H. Mamiya, I. Nakatani, and T. Furubayashi, *Phys. Rev. Lett.* **80**, 177 (1998).
- ¹⁴T. Jönsson, P. Nordblad, and P. Svedlindh, *Phys. Rev. B* **57**, 497 (1998).
- ¹⁵J. García-Otero, M. Porto, J. Rivas, and A. Bunde, *Phys. Rev. Lett.* **84**, 167 (2000).
- ¹⁶P. Allia, M. Knobel, P. Tiberto, and F. Vinai, *Phys. Rev. B* **52**, 15 398 (1995); or the more recent work in the context of spin-glass-like particle phases: B. Idzikowski, U. K. Rössler, D. Eckert, K. Nendov, and K.-H. Müller, *Europhys. Lett.* **45**, 714 (1999).
- ¹⁷E. Bonnetti, L. Del Bianco, D. Fiorani, D. Rinaldi, R. Caciuffo, and A. Hernando, *Phys. Rev. Lett.* **83**, 2829 (1999).
- ¹⁸J. A. De Toro, M. A. Arranz, A. J. Barbero, M. A. López de la Torre, and J. M. Riveiro, *J. Magn. Magn. Mater.* **231**, 291 (2001).
- ¹⁹M. F. Hansen and S. Morup, *J. Magn. Magn. Mater.* **203**, 214 (1999).
- ²⁰T. Bitoh, K. Ohba, M. Takamatsu, T. Shirane, and S. Chikazawa, *J. Phys. Soc. Jpn.* **64**, 1305 (1995).
- ²¹X. Batlle, M. García del Muro, and A. Labarta, *Phys. Rev. B* **55**, 6440 (1997).
- ²²J. A. Mydosh, in *Spin Glasses: An Experimental Introduction* (Taylor & Francis, London, 1993).
- ²³P. Jönsson, M. F. Hansen, and P. Nordblad, *Phys. Rev. B* **61**, 1261 (2000).
- ²⁴J. Zhang, C. Boyd, and W. Luo, *Phys. Rev. Lett.* **77**, 390 (1996).
- ²⁵J. L. Tholence, in *Magnetic Susceptibility of Superconductors and Other Spin Systems*, edited by R. A. Hein, T. L. Francavilla, and D. H. Liebenberg (Plenum, New York, 1991), p. 503.
- ²⁶D. Sherrington and S. Kirkpatrick, *Phys. Rev. Lett.* **35**, 1792 (1975); *Phys. Rev. B* **17**, 4384 (1978).
- ²⁷P. Nordblad and P. Svedlindh, in *Spin Glasses and Random Fields*, edited by A. P. Young (World Scientific, Singapore, 1997).
- ²⁸P. C. Hohenberg and B. I. Halperin, *Rev. Mod. Phys.* **49**, 435 (1977).
- ²⁹E. Obradó, A. Planes, and B. Martínez, *Phys. Rev. B* **59**, 11 450 (1999).
- ³⁰D. Fiorani, in *Studies of Magnetic Properties of Fine Particles and their Relevance to Materials Science*, edited by J. L. Dormann and D. Fiorani (Elsevier, Science, New York, 1992), p. 135.
- ³¹D. S. Fisher and D. A. Huse, *Phys. Rev. B* **38**, 497 (1998).
- ³²K. Jonason and P. Nordblad, *Physica B* **279**, 334 (2000).
- ³³C. Djurberg, P. Svedlindh, P. Nordblad, M. F. Hansen, F. Badker, and S. Morup, *Phys. Rev. Lett.* **79**, 5154 (1997).
- ³⁴D. Fiorani, J. L. Dormann, R. Cherkaoui, E. Tronc, F. Lucari, F. D'Orazio, L. Spinu, M. Nogues, A. García, and A. M. Testa, *J. Magn. Magn. Mater.* **196-197**, 143 (1999).
- ³⁵J. Kapoor, J. Andres, F. Mezei, Yi Li, C. Polaczyk, D. Riegel, W. D. Brewer, E. Beck, S. B. Legoas, and S. Frota-Pessôa, *Phys. Rev. Lett.* **77**, 2806 (1996).
- ³⁶M. B. Stearns and Y. Cheng, *J. Appl. Phys.* **75**, 6894 (1994).
- ³⁷For strong, weakly temperature dependent paramagnets like elements and alloys of the 3d, 4d, and 5d transition series (Pd below 300 K, for instance) typical values are about 10^{-6} emu/g. For example, 5×10^{-6} emu/g is found for pure Pd and 2×10^{-6} emu/g for alloys as V_3Ga or V_3Au . A completely temperature independent Pauli contribution would be associated with much lower values. On the other hand, a strong Curie contribution is not aparent in the low temperature M vs T curves, which do not show any upturn. From the high field slope of a hysteresis cycle measured at 5 K, we estimated an upper limit, $\chi_{PM}(5 \text{ K}) \leq 7 \times 10^{-5}$ emu/g. Such a Curie term would be less

relevant at 200 K, a simple estimation rendering $\chi_{PM}(200 \text{ K}) \leq 2 \times 10^{-6}$ emu/g. Attempts of including a paramagnetic term of reasonable magnitude ($\leq 10^{-5}$ emu/g) in the fits were unsuccessful.

³⁸G. F. Zhou and H. Bakker, Phys. Rev. B **48**, 13 383 (1993); B. Huang, N. Tokizane, K. N. Ishihara, P. H. Shingu, and S. Nasu,

J. Non-Cryst. Solids **117-118**, 688 (1990).

³⁹L. H. Lewis, M. J. Kramer, K. W. Dennis, and R. W. McCallum, J. Appl. Phys. **87**, 4735 (2000).

⁴⁰G. Le Caër, P. Delcroix, T. D. Shen, and B. Malaman, Phys. Rev. B **54**, 12 775 (1996).